ERANOS NEUTRONICS CALCULATIONS OF A $^{11}B_4C$ MODERATED SUBASSEMBLY AND EXPERIMENTAL VALIDATION IN MASURCA

G. Rimpault, R. Soule, J.F. Lebrat, M. Martini, J.P. Chauvin, R. Jacqmin
CEA, Cadarache
grimpault@cea.fr

P. Morris
BNFL, on attachment at CEA, Cadarache
peter@baobab3.cad.cea.fr

D. Biron, S. Janski
EDF/SEPTEN

D. Verrier
FRAMATOME

ABSTRACT

One of the potential solutions for the reduction of current nuclear waste stockpiles is the introduction, within a fast core, of heterogeneously positioned subassemblies dedicated to the burning of Americium. The ECRIX-B ($^{11}B_4C$) and ECRIX-H (CaH_2) moderated minor actinide (MA) target programmes in the PHENIX reactor are the first irradiations planned to include targets specifically designed for the 'burning' of americium. In order to provide a suitable preliminary database on such systems to validate existing design calculations, the COSMO-1 experimental programme (COSMO : **CO**nfigurations pour la **S**imulation de la **Mo**deration) in the MASURCA facility at CEA, Cadarache has included an $^{11}B_4C$ (^{11}B, 99.66%) moderated subassembly introduced at the centre of a critical configuration loaded with a typical fast reactor cell (MOX fuel 25% enriched). This paper documents an important part of the analysis of the results from this experiment and is the first stage of an ongoing series of activities focused on the validation of the ERANOS code and data system (ERANOS : **E**uropean **R**eactor **A**nalysis and **N**eutronic **O**ptimised **S**ystem) for the modelling of americium burning systems. The adopted solution is to use cell and spatial calculations with an explicit P1 description of the scattering law throughout the neutron transport calculation scheme. The adoption of such a scheme brings with it the requirement for

additional validation of both the revised calculational method and the nuclear data used in its execution. This paper presents evidence of the suitability of ERANOS for the modelling of $^{11}B_4C$ moderated target systems. To this end, associated critical masses, relative reaction rates and ratios have been calculated and compared to the COSMO-1 experimental values. Calculation results fall within the experimental error margins for the major isotopes showing evidence of a suitable representation of the neutron slowing down within the target and of the resultant power peak in the neighbouring fuel assembly. However, some of the minor actinide reaction rates are badly predicted suggesting deficiencies in the nuclear data for these isotopes.

1. INTRODUCTION

The COSMO experimental programme[1] is an ongoing series of three separate experiments designed to cumulatively provide a sound base of experimental neutronic data on the performance of various moderated sub-assemblies, heterogeneously positioned within a critical fast reactor core. Primarily, the data produced is for use in the continuing validation and development of the ERANOS neutronic code and data system[2] for application to the analysis of reactors containing such materials and, in particular, to validate existing and future calculations performed using ERANOS in support of the ECRIX-B ($^{11}B_4C$) and ECRIX-H (CaH_2) moderated minor actinide (MA) target programmes in the PHENIX reactor. The driving force behind the choice of such experiments and subsequent code development is the growing trend of research towards the implementation of systems for the incineration and transmutation (or 'burning') of MA and fission product wastes. In the case of fast neutron systems, the use of moderated regions around targets is considered in order to take advantage of the combination of the high fluxes available in a fast system together with the large reaction cross-sections available in the lower energy resonance and thermal spectrum regions.

The COSMO experimental programme contains three phases:

- The COSMO-1 phase contains an $^{11}B_4C$ (^{11}B, 99.66%) moderated subassembly introduced at the centre of a critical configuration loaded with a typical fast reactor fuel cell (MOX fuel 25% Pu fissile),
- The COSMO-2 phase, has the same $^{11}B_4C$ moderated subassembly located at the interface between the core and the fertile blanket and /or between the core and the steel reflector to simulate situations encountered in either a breeder reactor or a Pu burner reactor,
- The COSMO-3 phase, constitutes a parametric study of the more general moderated subassembly performed using a selection of moderators ($^{11}B_4C$, CaH_2, ZrH_2) and moderated zones of different sizes, in order to achieve a better understanding of the physics of the system and thus optimise the design.

The ERANOS code and data system contains features enabling suitable neutronics calculations for fast systems incorporating thermal or low energy spectrum regions. The adopted solution within ERANOS is to use cell and spatial calculations with an explicit P1 description of the scattering law throughout the calculation scheme. This paper presents some of the more significant elements of the neutronic validation for the COSMO-1 phase. To this end,

associated relative reaction rates and ratios have been calculated for the reference (COSMO-1_Reference) and moderated target (COSMO-1_M) cores, compared to the experimental values and conclusions drawn.

2. COSMO-1 EXPERIMENTAL PROGRAMME

2.1. REFERENCE CONFIGURATION (COSMO-1_REFERENCE)

Figure 1 presents an XY plane view of the COSMO-1 Reference core configuration. This configuration contained standard reflector/shield compositions and geometries together with fuel of 50% MOX (25% Pu fissile), 50% Na, distributed homogeneously throughout. The locations of the horizontal and axial canals through which traverse measurements were taken, are suitably marked.

2.2. $^{11}B_4C$ MODERATED TARGET CONFIGURATION (COSMO-1_M)

Figure 2 presents an XY plane view of the COSMO-1 $^{11}B_4C$ moderated target core. This core was formed by removal of fuel cells from the central target region and relocated at the core periphery with the addition of extra cells to achieve the appropriate level of criticality. Again, the locations of the radial and axial canals through which traverse measurements were taken are plainly visible. A detailed view of the target region itself is presented in figure 3.In this figure it can be seen that a central Na region is completely surrounded by a region of $^{11}B_4C$ which is in turn surrounded by a region of stainless steel (SS), designed to represent the ECRIX-B sub-assembly wrapper and acting as a localised reflector.

2.3. MEASUREMENTS

Measurements made for these configurations included assessment of Critical Mass, the reactivity change due to insertion of the moderated target via the MSA method together with horizontal/axial reaction rate traverses and subsequent spectral indices. Many of the measurements were performed identically for both the reference and the moderated configurations in order to provide suitable comparison from which to quantify important effects. The techniques used were based on absolute and relative fission rate measurements (using fission chambers) of the major actinides (^{235}U, ^{238}U, ^{239}Pu), the minor actinides (^{237}Np, ^{238}Pu, ^{240}Pu, ^{241}Pu, ^{242}Pu, ^{241}Am, ^{243}Am) and on activation techniques. For each configuration, the experimental method determines the neutron spectrum axially through the central core assembly and horizontally across the neighbouring subassemblies. Neutron counters placed at various positions both at the core periphery and within the core itself provided the means of reference for core reactivity calculations.

The reaction rate traverses and activation detector measurements had a dual function. Firstly, to provide information about the expected fast flux depression and the corresponding increase in low energy resonant flux (and hence transmutation rates) within the central sub-critical zone of the target assembly. Secondly, to locate the position of the power maxima in the nearest

neighbouring fuel sub-assembly induced by the moderated target and the resultant diffusion back into the fuel of slowed down neutrons. It is worth noting at this point that, as is shown in figures 1 and 2, the horizontal traverses were not in fact taken through the central target region itself but passed adjacent to this region, as close to the target as possible, through the nearest neighbouring sub-assembly. Spectral indices taken from the core centre, deduced from the above reaction rate measurements and made relative to ^{235}U fission, provided a convenient method to infer information about spectrum hardness.

3. CALCULATION SCHEME

The calculation scheme adopted was that of the pre-defined Reference Route involving initial ECCO cell calculations[3] (ECCO : **E**uropean **C**ell **CO**de) target and surrounding regions followed by expansion with spatial calculation over the whole core. The cell calculation was performed using the 33 broad group scheme expanded to 1968 groups for a fine group step to incorporate resonance region cross-section information.
Final condensation was to 33 groups for application in the spatial calculations. Based on extensive past experience, the use of such a scheme was considered suitable for the reference configuration (COSMO-1_REFERENCE) configuration. Similarly, the same scheme, as will be demonstrated in the results section, was deemed suitable for use with the $^{11}B_4C$ moderated configuration (COSMO-1_M) .

The choice of geometries used for both cell and whole core calculations was dependant upon the degree of heterogeneity involved. For the reference case, 2D RZ cylindrical geometries, an efficient approach to adopt for such a homogeneous and symmetric configuration, were used throughout the main cell and spatial calculations utilising P1 transport and S8 scattering approximations. A 3D XYZ nodal transport code calculation[4] was used for the evaluation of the critical mass.

As can be seen in figure 3, for the $^{11}B_4C$ moderated target core, the target region is significantly asymmetric and a high degree of anisotropy in the flux and scattering was expected. Consequently, it was necessary to improve the representation and the cell calculation for the moderated, sub-critical target core was performed using a 2D, XY geometry, critical macrocell approach. Detailed modelling within the inner target was maximised to enable a suitable calculation of the steep flux gradients expected in this region. Spatial calculations were performed in both 2D, RZ cylindrical and 2D XY geometry to provide axial and horizontal traverse data respectively. Cell and spatial calculations were performed using the P1 transport and S8 scattering approximations. The critical mass was evaluated, as for the reference case, by the use of a separate 3D XYZ nodal transport code calculation.

4. RESULTS

4.1. CRITICAL MASSES AND REACTIVITY CHANGE

Table 1 presents the results of the critical mass calculations for both the reference and moderated target configurations. In this table, modelling corrections for the core and reflector regions[5] were applied as necessary.

Table 1 COSMO-1 Critical Mass Calculation

	REFERENCE CASE	B4C TARGET CASE
Keff, RZ Bistro Transport P1	0.99966	0.99751
Initial Reactivity (pcm)	-36	-250
Modelling Corrections (pcm)	-118	118
Corrected Keff (calc)	0.99846	0.99869
Corrected Reactivity (calc) (pcm)	-154	-131
Keff (exp)	0.99856	0.99927
Reactivity (exp) (pcm)	-144	-73
C-E (pcm)	-10	-59

As can be seen, the reference calculation has produced a very small discrepancy of -8 pcm with respect to the experimental value. Calculational uncertainties for the similar reference core of ZONA2B have already been evaluated giving an uncertainty due to nuclear data alone of around ±300pcm. For the moderated target case, the discrepancy is increased slightly to -58 pcm, due to the effect on calculation caused by the inclusion of moderator but is still small compared with the uncertainty due to nuclear data. From these results, we can conclude that the ERANOS computed critical mass agrees with the experimental values, the discrepancies falling well within the quoted uncertainties.

Table 2 below presents the results of calculation for the subassembly reactivity worth.

Table 2 $^{11}B_4C$ Target Reactivity Worth

B4C MODERATED SUBASSEMBLY REACTIVITY WORTH			
Calculated Value (pcm)	**MSA Experimental Value (pcm)**	**MSM Corrected Experimental Value (pcm)**	**C-E (pcm)**
-1972	-1690	-1862	-110

Here the discrepancy after calculation of the experimental result by the MSA method and subsequent correction by MSM method is larger than the discrepancy for the overall critical mass (see table 1) indicating that the calculation in the target region itself may be responsible for the increased discrepancy on critical mass for the moderated core. This situation is better understood if one considers the strong changes across the target in isolation. Figure 4 presents a comparison of calculated neutron spectra in 33 groups at three points, positioned radially across the target region. In this figure it can be seen that there is a significant softening of the spectrum in the fuel adjacent to the target which, as we will see later, will result in some localised increase of power in this area. It is clear that the spectrum is softened considerably over the moderated region with a large integral increase of flux over resonance energies, between group 12 and group 25, leading to a reduction in the higher group fluxes. Most of this change is carried over into the inner Na zone with little or no further change. Note that there is no apparent change in the thermal region fluxes and the modified spectrum is still strongly epi-thermal. A direct result of this shift of spectrum across the target is an increase in calculated resonant region reaction rates as typified by ^{243}Am capture. Figure 5 presents a graph of the normalised reaction rate for ^{243}Am(n, γ)^{244}Am calculated radially across the whole of the moderated target core. Here, the effect of the increase in resonant region flux is clearly visible as a steep change in reaction rate. Naturally, the above situation implies higher actinide transmutation rates would be significantly increased inside the target region.

4.2. SPECTRAL INDICES

Table 3 below presents a comparison of discrepancies between calculated and experimental spectral indices taken at the centre of the cores for the two cases of interest. Note that the core centre for the moderated target case is located in the central Na region.

Table 3 Spectral Indices (C-E)/E for Reference and $^{11}B_4C$ Moderated Target Cases.

Reaction Chamber		REFERENCE CASE	B4C TARGET CASE
	Experiment Uncertainty @2sigma	(C-E)/E	(C-E)/E
U 238 (n,f)	±3%	-1.2%	-2.5%
Np 237 (n,f)	±3%	-3.5%	-9.3%
Pu 238 (n,f)	±5%	7.5%	11.8%
Pu 239 (n,f)	±2.5%	0.6%	-2.0%
Pu 240 (n,f)	±4.5%	2.7%	-0.2%
Pu 241 (n,f)	±4%	0.1%	-3.7%
Pu 242 (n,f)	±4.5%	-2.1%	-7.7%
Am 241(n,f)	±4.5%	7.7%	0.5%
Am 243(n,f)	±4.5%	5.1%	-5.2%

Firstly, although they are not presented here, the calculated values for spectral indices did confirm the measured spectrum shift over the moderated target assembly. Now, in table 3, consider the comparison of (C-E)/E for indices measured by reaction chamber. It is apparent that for the cases where the cross-section data is well defined (i.e. adjusted pointwise over many energy groups) such as for ^{235}U, ^{238}U, ^{239}Pu most other isotopes of Pu and ^{10}B, the indices are well predicted for both configurations with discrepancies generally lying well within the experimental uncertainties. This situation gives confidence that the fluxes (Figure 4) for both cases, but in particular those for the moderated target case, are reasonably well predicted. However, for the cross-sections where the data is sparse over many groups and current estimated data uncertainties are known to be large (particularly, ^{238}Pu and $^{241/243}Am$), there is systematic error with some consistently large discrepancies in evidence for both configurations. This suggests that the data needs improvement for these isotopes over resonant energies. The change in sign of the discrepancy for ^{243}Am fission between the two configurations coupled with the apparent increase in resonant region fluxes in the target region (figure 4) indicates that there may be an effect due to insufficient information relating to the shape of the cross-section function in the resonance region.

4.3. REACTION RATE TRAVERSES AND LOCALISED POWER PEAKING

Figures 6, 7 and 8 show a series of experimental and calculated fission reaction rate traverses all taken across the same horizontal canal (see figures 1 and 2) running immediately adjacent to the core central target assembly region. As noted earlier, the primary function of the horizontal traverse measurements in the moderated target core was to identify the location of the expected power peak in the nearest neighbour standard fuel sub-assembly caused by the build-up of slowed down neutrons diffusing back into the fuel region from within the moderated target. For the axial traverses, all passing through the central Na target region, peak power had been confirmed by experiment as being located in the central plane of the core and this has been satisfactorily reproduced in calculation. The horizontal traverses, enabled the location of the power peak in the fuel, within that central plane, to be identified. Figure 6 presents a comparison of horizontal traverses for ^{235}U fission rate for both the reference case and the $^{11}B_4C$ moderated target case. In this figure the increase in reaction rate in the vicinity of the target assembly (which is centred at the origin of figures 6, 7 and 8) as compared with the reference case is easily visible and well predicted by calculation. The total width of the moderated target region on these figures is approximately 12 cm, so it is clear that the change in reaction rate gradient commences well outside the target region. Figure 7 presents a similar traverse taken for ^{238}U fission. Here the expected lower response for the threshold reaction of ^{238}U fission, due to the softening of the spectrum in the target region, is apparent. Again, the experimental measurements are well reproduced by calculation. It should be noted that (C-E)/E values for both ^{235}U and ^{238}U at the centres of these traverses are around 2% and thus are of the order of the random uncertainty associated with the measurement. For the COSMO-1 cores, which as stated above are made up of mainly Pu fuel with only a trace of ^{235}U, the more significant traverse with respect to power peaking is that for ^{239}Pu fission rate. Figure 8 presents the traverse for this key reaction. As can be seen, the power peak is still visible in the central target region. Calculated values are again well representative of the experimental case.

The deviation between calculation and experiment apparent at the edge of the core (around ± 45 cm) is the result of reflector based modelling phenomenon affecting calculations of reaction rates at these neutron energies and is currently under investigation at CEA.

Figure 9 shows a graph of (C-E)/E values (%) for this traverse, where it can be seen that the discrepancy on the reaction rate, and hence power, in the important central region is less than 1% and in the core as a whole (neglecting the reflector based effects towards the core edge) does not really exceed around 2% at any point. The fluctuations apparent in this graph are the result of the positioning of structural materials (tube wrappers, brackets etc) overlapping the traverse points for the experimental measures. These structures were not explicitly modelled for the spatial calculations, hence there is some slight variation on the discrepancies at these points . Finally figure 10 presents a calculated lateral traverse taken in the central plane of the core but perpendicular to the horizontal canal. This traverse, which has points in the central fuel region coincident with the actual positions of the fuel/Na pins, clearly identifies the location of the maxima for ^{239}Pu fission in the moderated target core to be in the position of the nearest neighbour fuel pin. Note that this figure does not indicate any reaction rates in regions which do not contain fuel (i.e within the target or reflector).

CONCLUSIONS

In order to provide a suitable preliminary database on the neutronic performance of moderated sub-assemblies designed to burn americium from which to validate existing calculations[6], the COSMO-1 experimental programme in the MASURCA facility at CEA, Cadarache has been successfully completed. The programme configurations included an $^{11}B_4C$ (^{11}B, 99.66%) moderated subassembly placed at the centre of a critical core loaded with a typical fast reactor cell (MOX fuel 25% enriched). This paper documents significant elements of the analysis of results from this experiment and is the first stage in an ongoing series of activities focused on the validation of the ERANOS code and data system for the modelling of americium burning systems.

To this end, we have demonstrated here that the calculational scheme used within ERANOS is able to suitably reproduce the COSMO-1 experimental values for critical mass, reaction rates of key interest across the core and subsequent spectral indices to within experimental uncertainties for isotopes for which the available nuclear data is well defined. Additionally, the code has successfully predicted the location of the power peak induced by the moderated target in the neighbouring fuel assemblies and has confirmed its magnitude to within a few percent of the experimental value.

REFERENCES

1. R Soule et al, “The COSMO Experiments in the MASURCA Facility”, ANS Winter Meeting, Long Beach, California, USA, 14-18 November, 1999.

2. J.Y. Doriath, C.W. McCallien, E. Kiefhaber, U. Wehman, J.M. Rieunier, “ERANOS 1: The Advanced Sysyetm of European Codes for Reactor Physics Calculations”, International Conference on Mathematical Methods and Super Computing in Nuclear Computations, Karlsruhe, Germany, April 19-23, 1993.

3. M.J. Grimstone, J.D. Tullet, G. Rimpault, “Accurate Treatment of Fast Reactor Fuel Assembly Heterogeneity with the ECCO Cell Code”, International Conference on the Physics of Reactors: Operation, Design and Computation - PHYSOR 90, April 23-27, 1990.

4. E.E. Lewis and G. Palmiotti, “Simplified Spherical Harmonics in the Variational Method”, NSE 126, 48-58, 1997.

5. J C Bosq, ‘Développement et Qualification d’un Formulaire Adapté à SUPERPHENIX avec Réflecteurs’, THESE en Physique et Modélisation des Systèmes Complexes, Université de Provence (Nov 1998).

6. C. de StJean et al, “Uncertainties Associated with the use of the ERANOS Code System when Applied to the Moderated ECRIX Irradiation in the PHENIX Fast Reactor”, PHYSOR 2000, Pittsburgh, USA, May 2000.

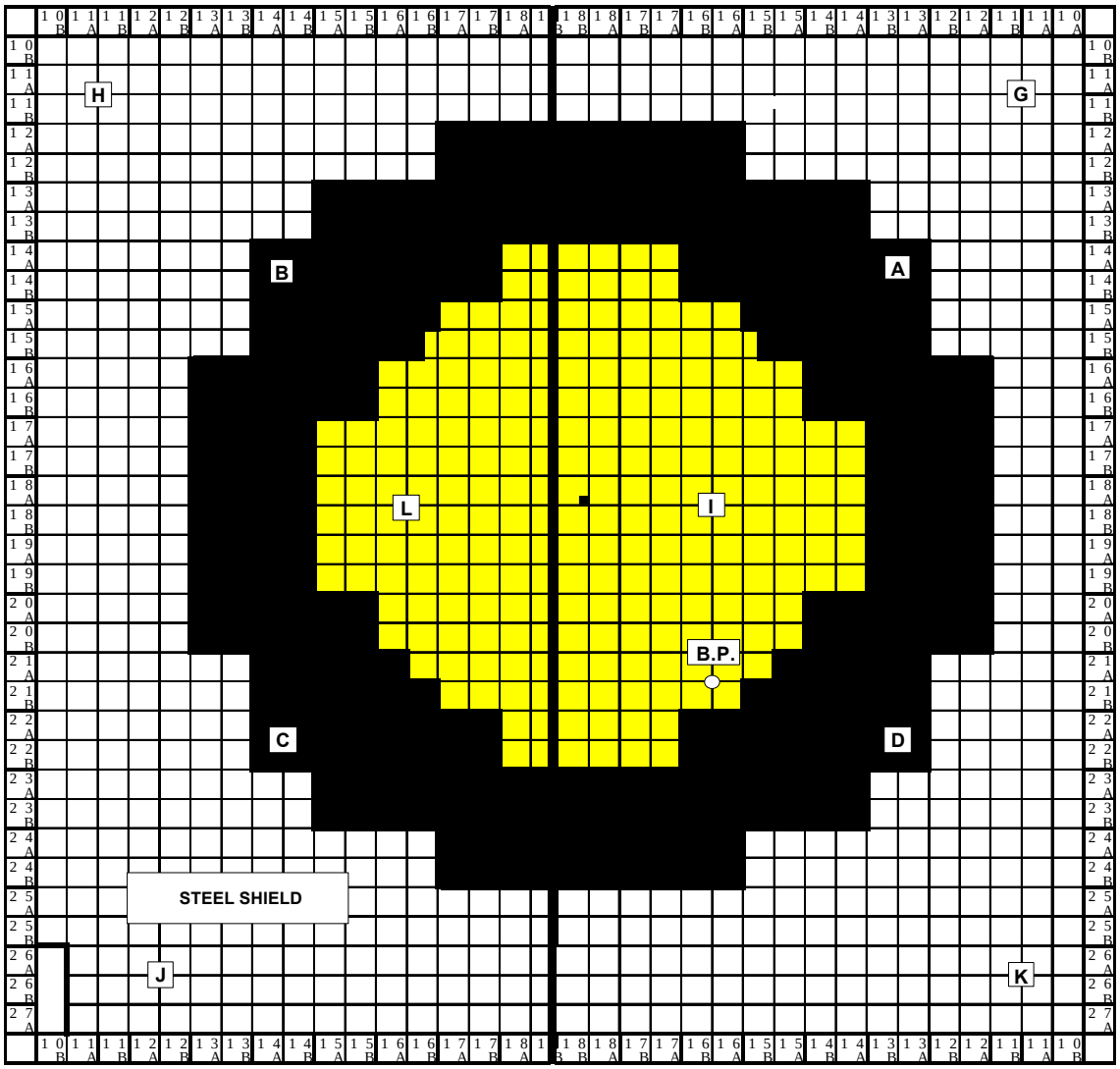

COSMO1_Reference Configuration (924 cell. PIT)

Reflector Tube Na/SS

Fuel Tube ZONA2PIT
Na/UO_2 - PuO_2

FIGURE 1 Plan View, COSMO-1_REFERENCE

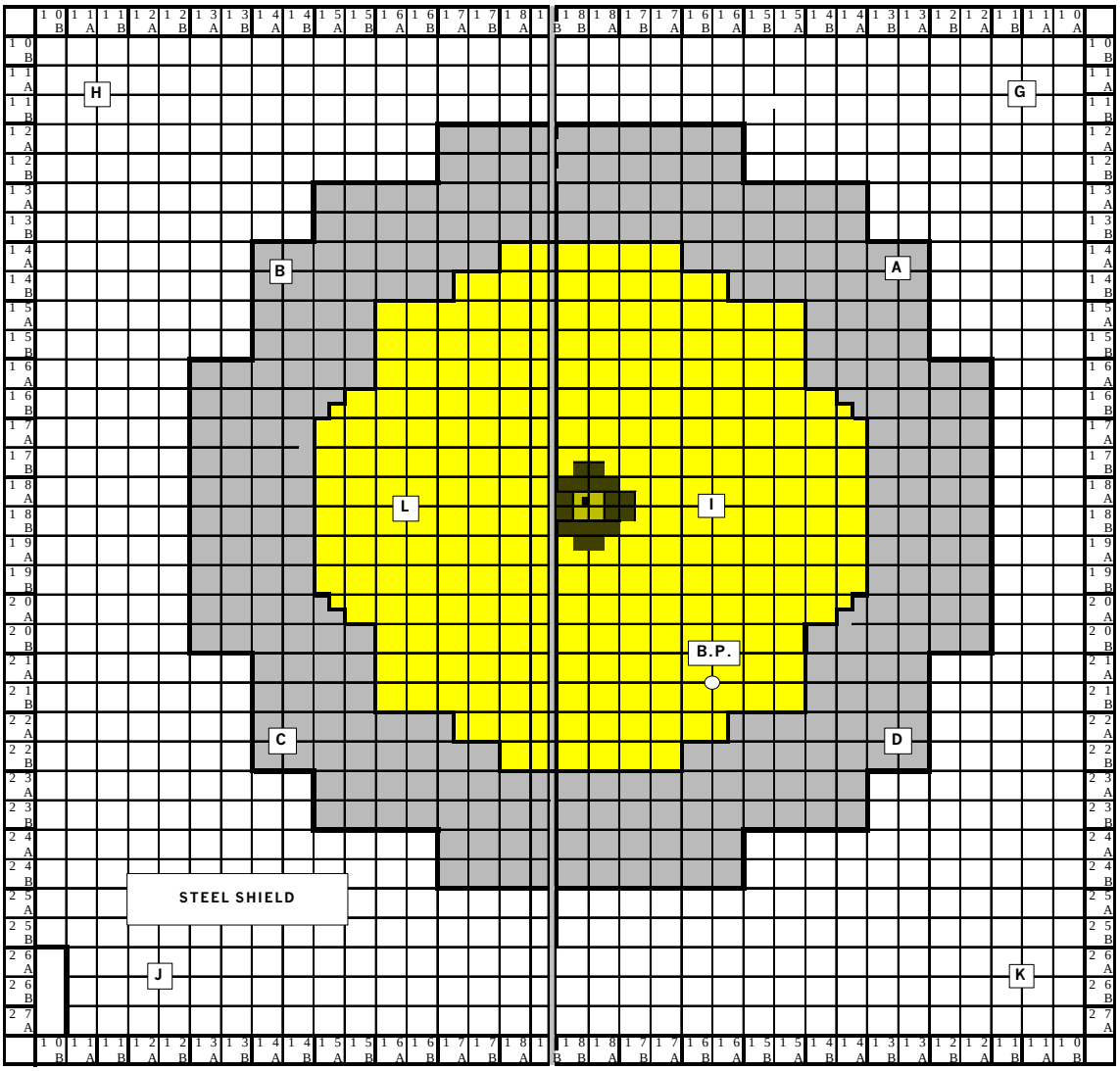

COSMO1_M (999 cell. PIT)

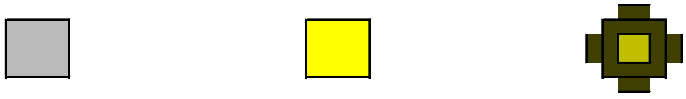

Reflector Tube Na/SS

Fuel Tube ZONA2PIT
Na/UO_2 - PuO_2

Moderated Target

FIGURE 2 Plan View, COSMO-1_M ($^{11}B_4C$ Target)

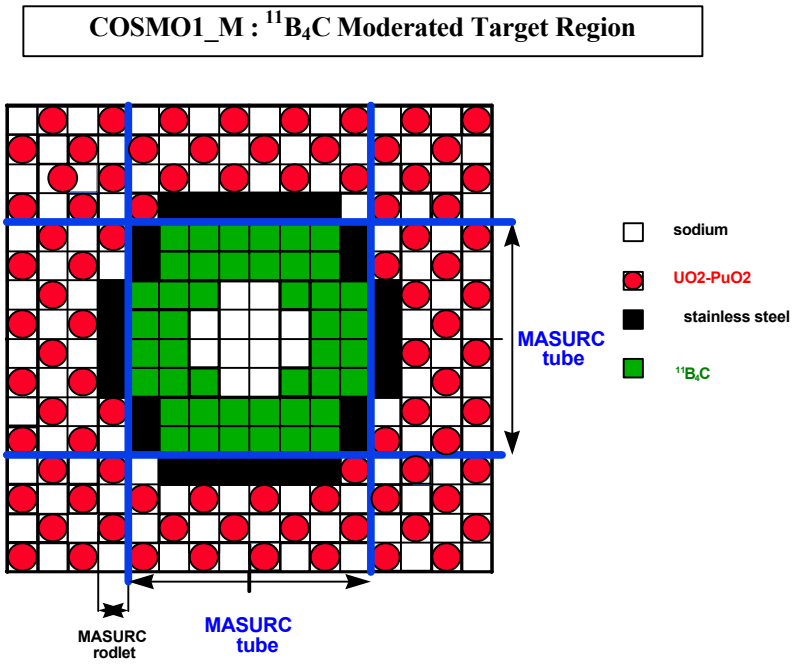

FIGURE 3 Detailed $^{11}B_4C$ Target View, COSMO-1_M

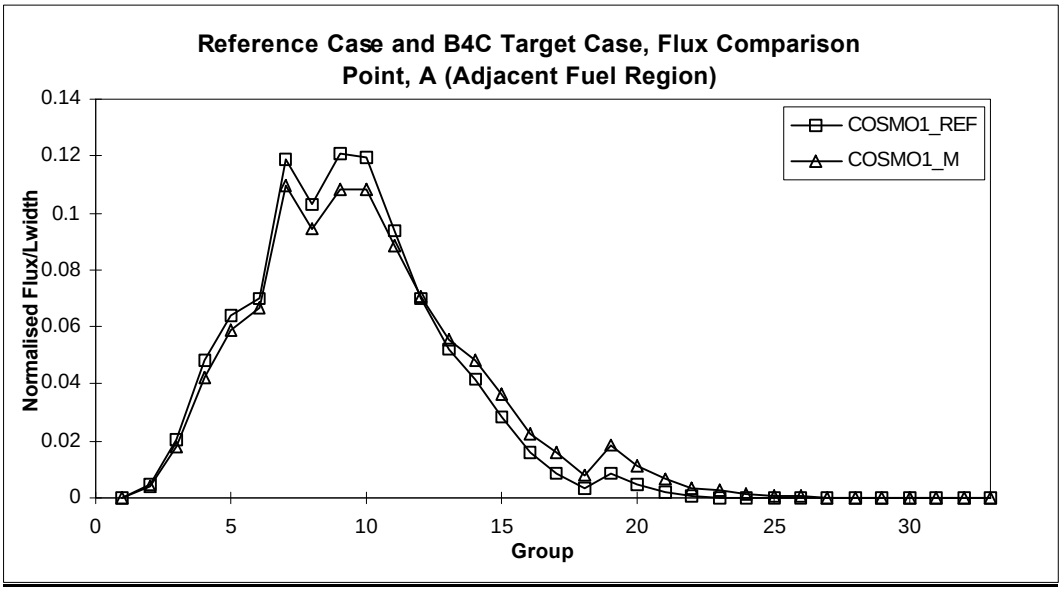

FIGURE 4 Pointwise Flux Comparison over Target Region (followed)

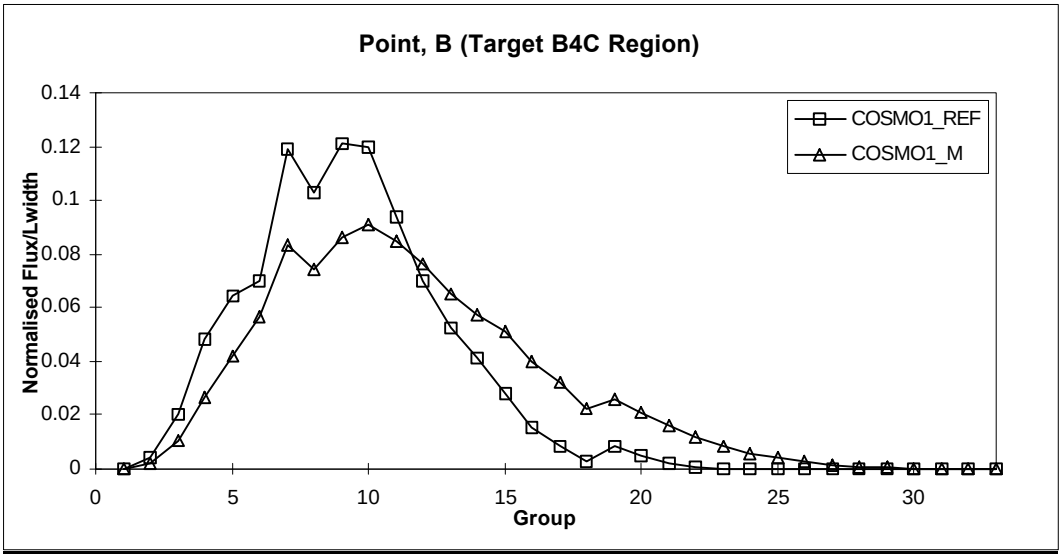

FIGURE 4 Pointwise Flux Comparison over Target Region (followed)

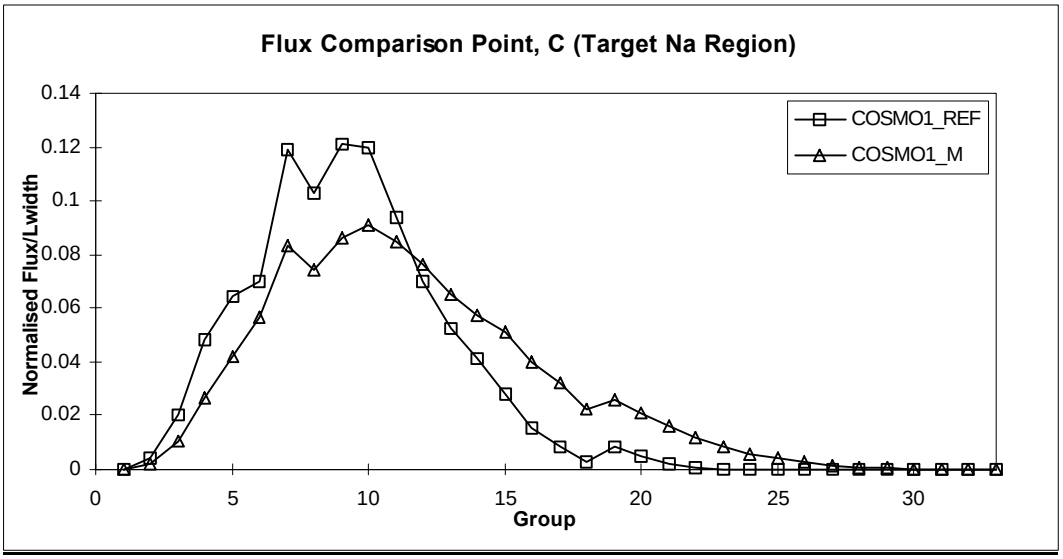

FIGURE 4 Pointwise Flux Comparison over Target Region (followed)

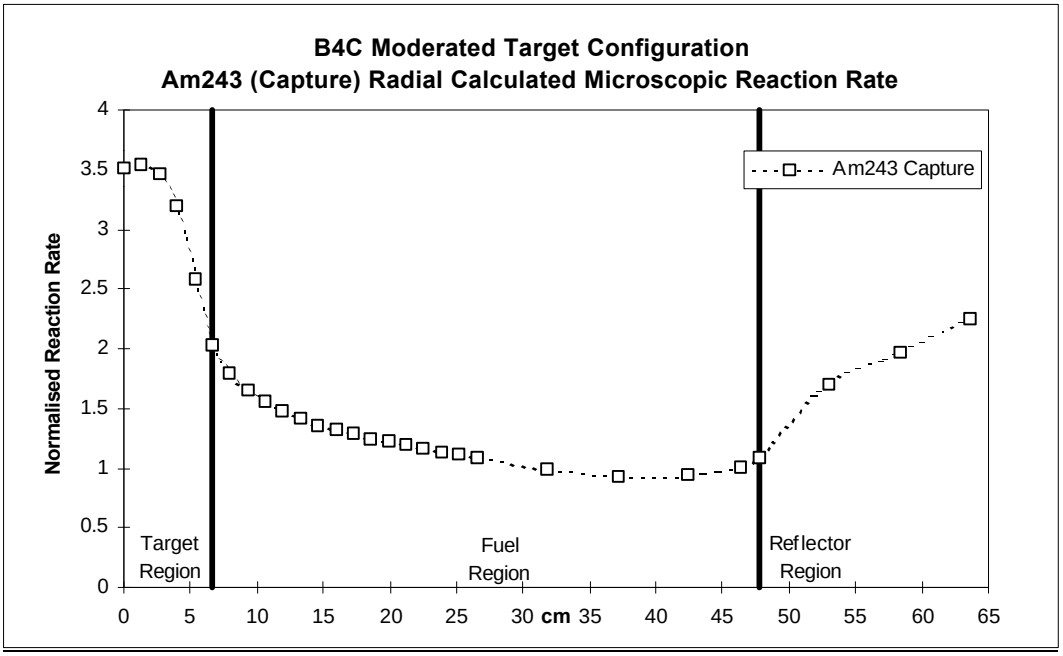

FIGURE 5 Radial Traverse, ^{243}Am Capture Rate

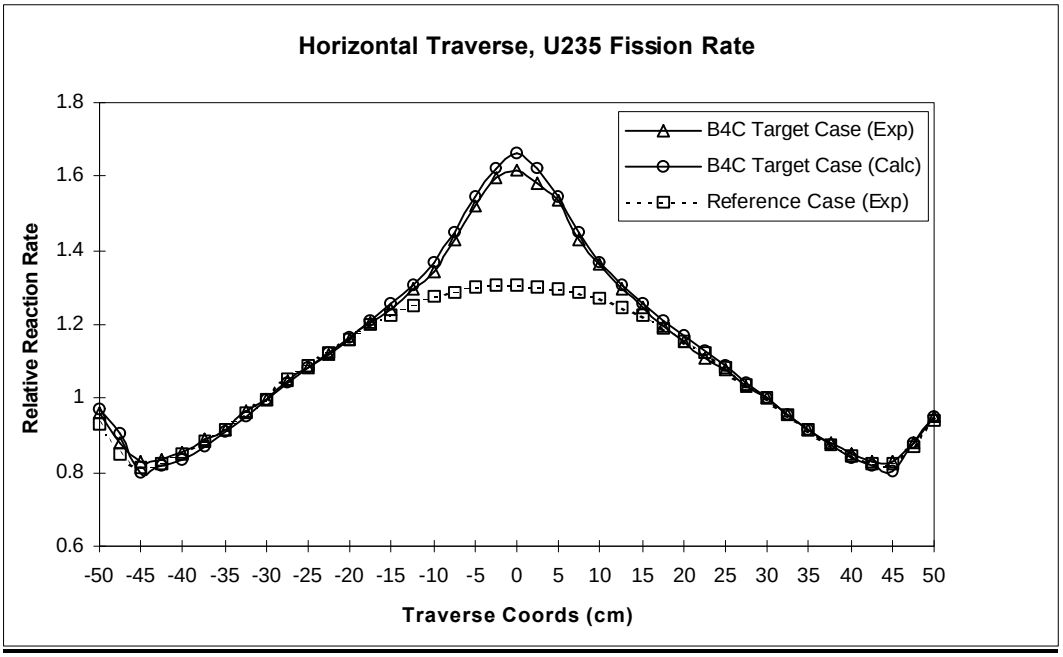

FIGURE 6 Horizontal Traverse, ^{235}U Fission Rate

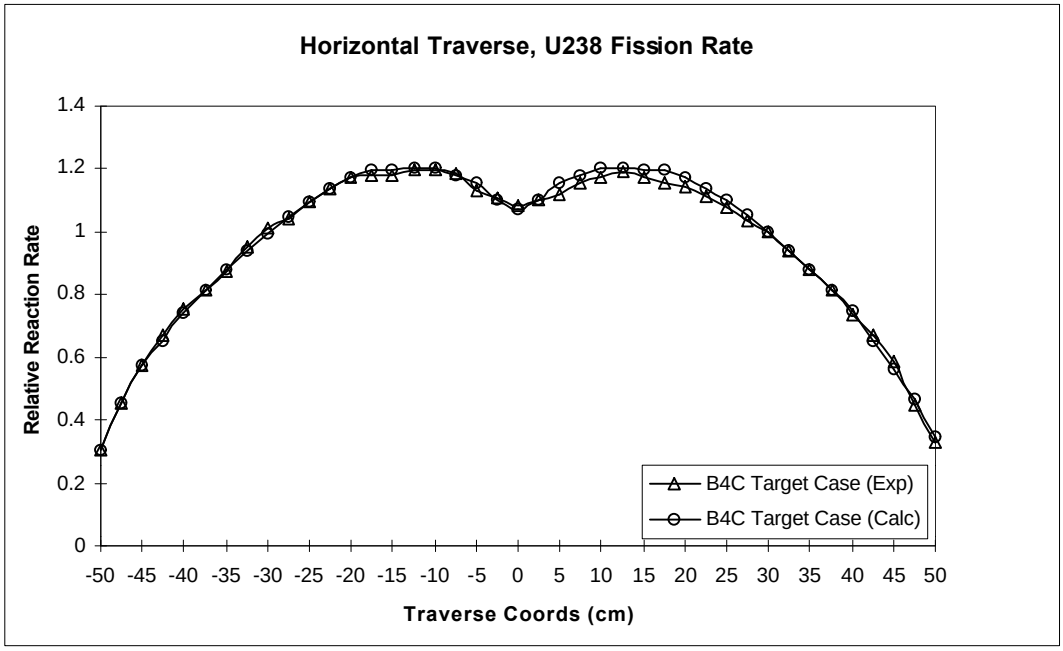

FIGURE 7 Horizontal Traverse, ^{238}U Fission Rate

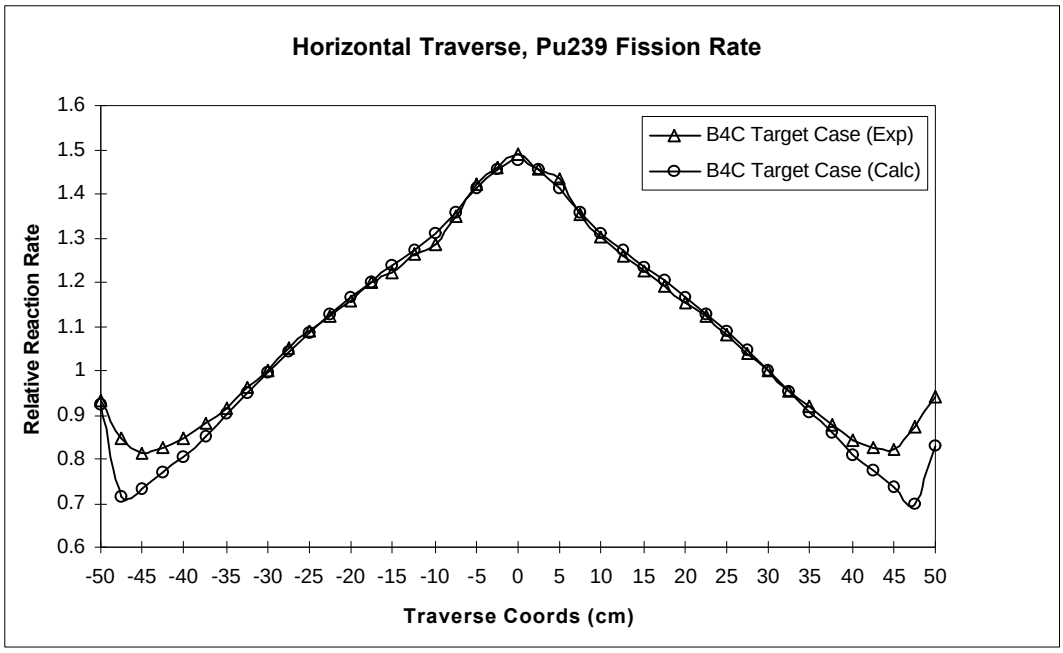

FIGURE 8 Horizontal Traverse, ^{239}Pu Fission Rate

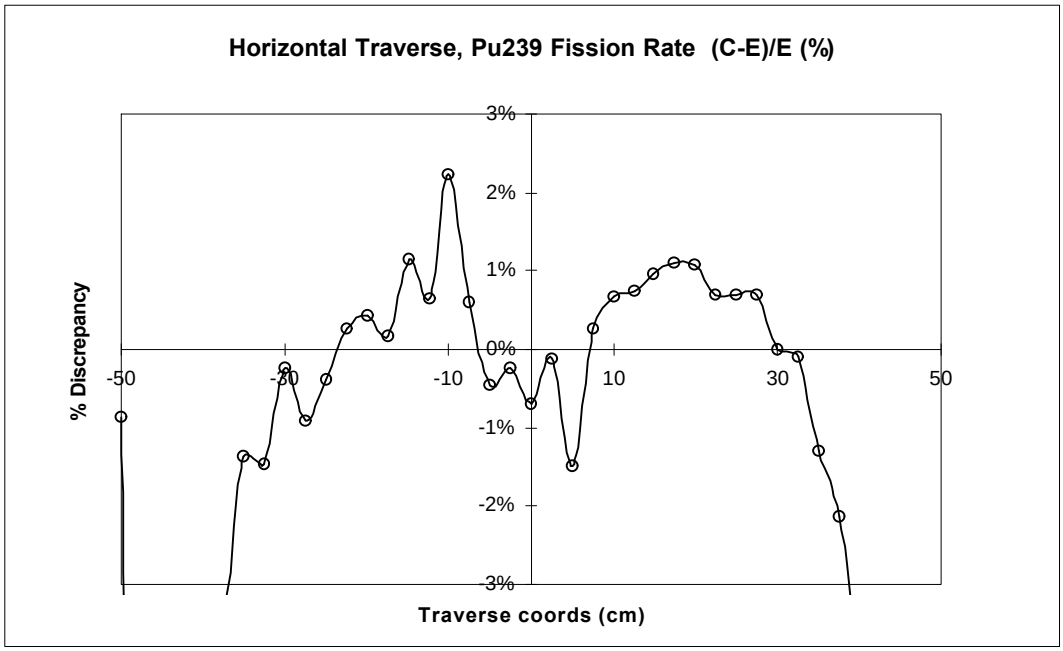

FIGURE 9 Horizontal Traverse, ^{239}Pu Fission Rate (C-E)/E

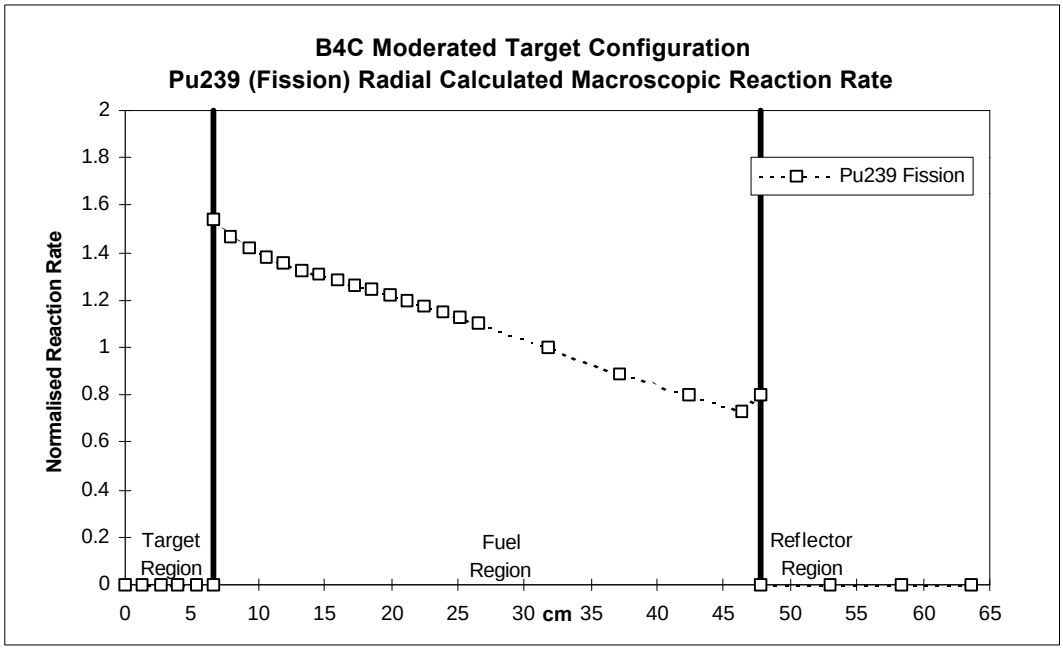

FIGURE 10 Radial Traverse ^{239}Pu Macroscopic Fission Rate